Support Information

Enantiomerselective sensing and light response of chiral molecule coated persistent luminescent material

Wenyan Zhang[a,*], Jing Li[a], Gongxuan Lu[b] Hangmin Guan[a], Lingyun Hao[a]

[a]College of Material Engineering, Jinling Institute of technology, Nanjing 211169, China

[b]State Key Laboratory for Oxo Synthesis and Selective Oxidation, Lanzhou Institute of Chemical Physics,

Chinese Academy of Science, Lanzhou 730000, China

*Corresponding author: E-mail: wiseyanyan@jit.edu.cn

1 Experimental detail

1.1 *Preparation of $Pr^{3+}:CaTiO_3$*

Herein, the $Pr^{3+}:CaTiO_3$was synthesized by sol-gel method. Typically, 5 mL tetrabutyl titanate (AR) and 15 mL anhydrous ethanol were mixed by ultrasonicating for 30 min, which was named solution A. Then calcium nitrate tetrahydrate (AR), praseodymium nitrate hexahydrate (AR) and 0.6 g boric acid were mixed in 7 mL anhydrous ethanol which contained 1 mL distilled water, and the mixture was named solution B. It should be noted that the molar ratio of Ca to Ti elements in solution A and solution B was kept 1:1, while that of Pr^{3+} to Ti elements was kept 0.002:1. Under magnetic stirring, solution B was slowly added into solution A.After that, 0.1 mL HCl was added into the mixture of A and B to accelerate the formation of sol, which was then kept at room temperature for 90 minutesand dried at 80 °C overnight. The obtained gel was calcinated at 1300 °C for 4 h to obtain $Pr^{3+}:CaTiO_3$powders, which were then grinded in agate mortar.

1.2 *Preparation of $Pr^{3+}:CaTiO_3@Ag$*

Ag nanoparticles were assembled on the surface of $Pr^{3+}:CaTiO_3$conveniently by silver mirror reaction to construct $Ag/Pr^{3+}:CaTiO_3$heterojunction. Firstly, analytical grade chemicals were purchased from Sigma-Aldrich andused without further purification.In a typical procedure, 1 mmol $AgNO_3$ was dissolved into100 ml distilled water at room temperature to form 0.01 M $AgNO_3$aqueous solution. Ammonia, which was diluted to 2%, was added drop by drop slowly until the white precipitation was totally dissolved to obtain silver-ammonia complex solution.

Then, 0.01mol glucose was dissolve into the prepared 100ml silver-ammonia complex solution by magnetic stirring. After that, 0.2 g grinded Pr^{3+}:$CaTiO_3$powders were dispersed in 50 mL silver-ammonia complex solution which contains glucose by ultrasonicating, and heated in the solution at 60°C for 60 min under magnetic stirring. During this process, Ag^+ ions were reduced to metallic state and the reduced product, Ag nanoparticles, were connected on the surface of Pr^{3+}:$CaTiO_3$After the silver mirror reaction, the products were filtered and washed several times with distilled water.

1.3 *Preparation of Pr^{3+}:$CaTiO_3$@Ag@L-cysteine*

L-cysteine monolayer was linked toPr^{3+}:$CaTiO_3$@Ag by impregnation method. In a typical synthesis,0.2g Pr^{3+}:$CaTiO_3$@Ag was ultrasonically dispersed into 20 mL L-cysteine aqueous solution (concentration of 20 mM). The dispersion was then incubated in N_2 atmosphere for24 h to achieve equilibrium state. L-cysteinemolecules were attached robustly onto Pr^{3+}:$CaTiO_3$@Agsurface due to the formation of Ag-S bonds and hydrogen bonds, as well as the electrostatic interaction between the molecules and Pr^{3+}:$CaTiO_3$@Ag.

1.4 *Characterization Details*

1.4.1 Structure, elements and morphology analysis

X-ray diffraction (XRD) patterns of the samples were recorded on a Rigaku B/Max-RB diffractometer with a nickel filtrated Cu Kα radiation operated at 40 kV and 40mA. The SEM images were recorded by Hitachi SU 8010 electron microscope with INCA X-Act EDS probe. X-ray photoelectron spectroscopy (XPS) analysis was performed using a VG Scientific ESCALAB210-XPS photoelectron spectrometer with an Mg Kα X-ray resource. X-ray photoelectron spectroscopy (XPS)was performed using a VG Scientific ESCALAB 210-XPS photoelectron spectrometer. Base pressure of the UHV chamber was $5*10^{-9}$ Torr and Mg Kα X-ray (300W, 1253.6 eV) was used as the X-ray resource. The pass energy was 100 eV for wide range scans (survey), and 20 eV for high resolution measurements. The energy step was 1 eV for survey scans, while high resolution measurements were recorded with 0.1 eV energy step. The binding energies were referenced to the C 1s level at 284.6 eV for adventitious carbon [32]. The samples were pressed into thin sheets on Al aluminum foils. Before loading the foils into XPS analyzing chamber, they were evacuated ($5*10^{-5}$ Torr) for 24 h to remove the moisture and adsorbed impurity on their surface. The binding energy was selected by choosing the maximum

intensity value at each peak.

1.4.2 Electrochemical characterization and light-response measurement

The enantiomerseletive sensing of working electrode was carried out from -1 V to 1 V in 25 mL electrolyte containing 20 mM L-Arginine and 50 mM KCl, as well as 25 mL electrolyte containing 20 mM D-Arginine and 50 mM KCl, respectively. Pt electrode was used as the counter and calomel electrode as the reference. The CV scanning rate was 50mV/s and 100 mV/s. The working electrode was coated by equal amounts ofPr^{3+}:CaTiO$_3$@Ag and Pr^{3+}:CaTiO$_3$@Ag@L-cysteine.

In terms of light-response detection, CV scanning was conducted in 20 mM D-Arginine electrolyte with 50 mM KCl, scanned at the rate of 50mV/s. Photocurrent was measure with the illuminating of 365 nm UV light of 5W, and dark current was detected without light irradiation. As for the open circuit potential measuring, the electrolyte was 0.1 mol/L Na_2SO_4 solutions. The fluorescence spectra and decay time were measured by Edinburgh Instruments FS5 Spectrofluorometer operating in Multi-Channel Scaling mode (MCS) with the capability to measure sample decays with lifetimes of over one microsecond.

1.4.2 H_2O_2 detection

The formation of H_2O_2 was measured by spectrophotometric titration of the used electrolytes, with the o-tolidine as redox indicatorand0.1 M Na_2SO_4 as solvent. If $H_2O_2$was produced, a yellow color appearedwith an absorption peak at about 436 nm. This peak is characteristic for the complete two-electron oxidation product of o-tolidine formed by the reaction with hydrogen peroxide. The detection steps are as follows. (1) Keepthe anode coated with Pr^{3+}:CaTiO$_3$@Ag or Pr^{3+}:CaTiO$_3$@Ag@L-cysteine at a constant potential of1.5 V (vs calomel) for 30 min in 0.1 M Na_2SO_4 electrolyte. (2) Take out 4 mL electrolytes near anode by 1 mL pipette, then add 1 mL o-tolidine and mix them by vibrating. (3) After 30 min, measure the absorption spectra of the solutionby a Varian Cary 50 Bio UV/ Visible spectrophotometer.

2 Characterizations

2.1 Electrons lifetime

Tab. S1 Electrons lifetime of Pr^{3+}:$CaTiO_3$, Pr^{3+}:$CaTiO_3$@Ag and Pr^{3+}:$CaTiO_3$@Ag@L-cysteine

Sample	$\tau 1$ (μs)	$\tau 2$ (μs)	χ^2
$CaTiO_3$,Pr^{3+}	55.4	424.9	1.01
$CaTiO_3$: Pr^{3+}@Ag	54.5	337.5	1.04
$CaTiO_3$: Pr^{3+}@Ag@L-cysteine	50.4	151.4	1.03
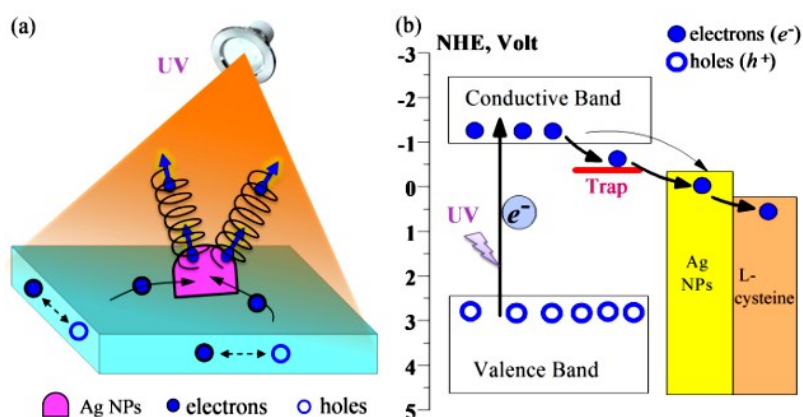
Scheme S1 Proposed photocatalytic mechanism for hydrogen evolution over Pr^{3+}:$CaTiO_3$@Ag@L-cysteine under visible light irradiation

2.2 Supplemental information of Pr^{3+}:$CaTiO_3$
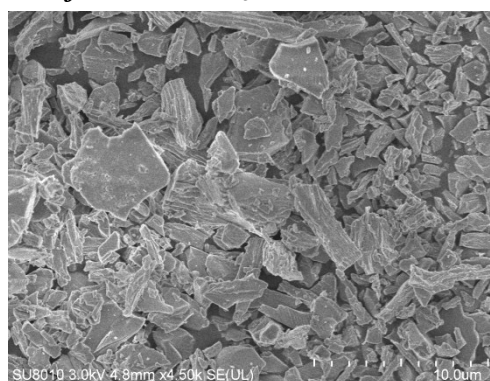
Fig. S1 SEM image of Pr^{3+}:$CaTiO_3$
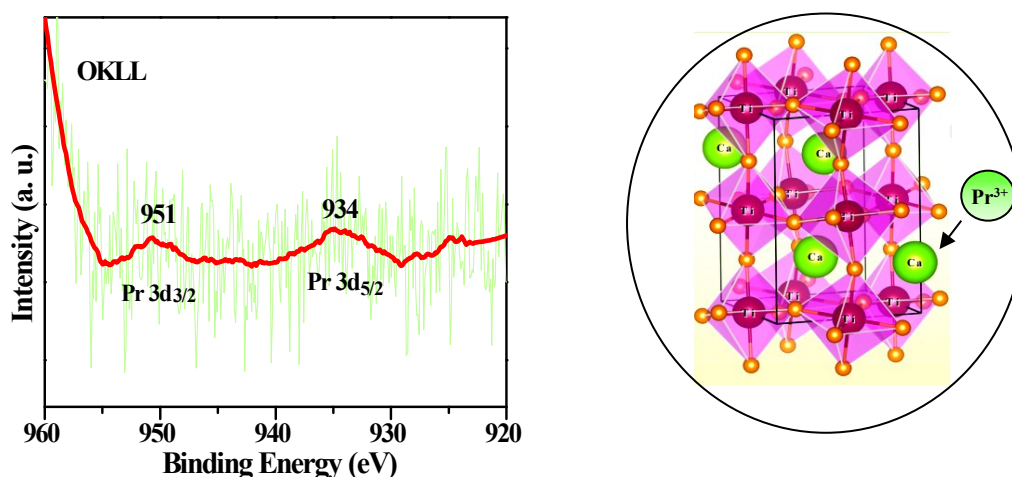
Fig. S2 Pr 3d XPS spectrum of Pr^{3+}:CaTiO$_3$**Scheme S1** Doping of Pr^{3+} ions in CaTiO$_3$

Fig. S1 and Fig. S2 show the morphology and Pr 3dXPS spectrum of Pr^{3+}:CaTiO$_3$. It can be seen from Fig. S1 that the morphology of Pr^{3+}:CaTiO$_3$ is not uniform, and there is no white dots connected on the surface Pr^{3+}:CaTiO$_3$ before assembling them with Ag nano-particles. The Pr element signal in Fig. S2 stems from the doping of Pr^{3+} ions in the lattice of CaTiO$_3$, which generate traps in CaTiO$_3$ lattice for the storing of long-lifetime photo electrons, as illustrated in Scheme S1.
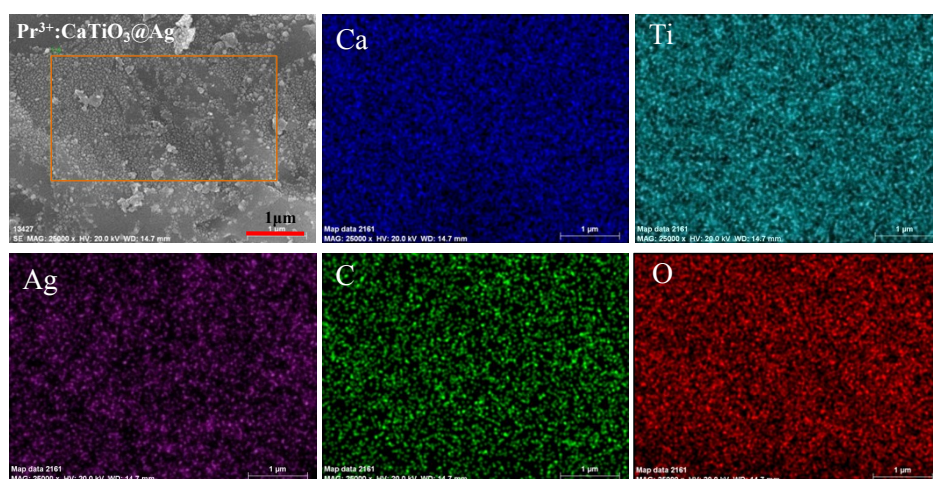
2.2 Supplemental information of Pr^{3+}:CaTiO$_3$@Ag

Fig. S3 Elemental Mapping ofPr^{3+}:CaTiO$_3$@Ag
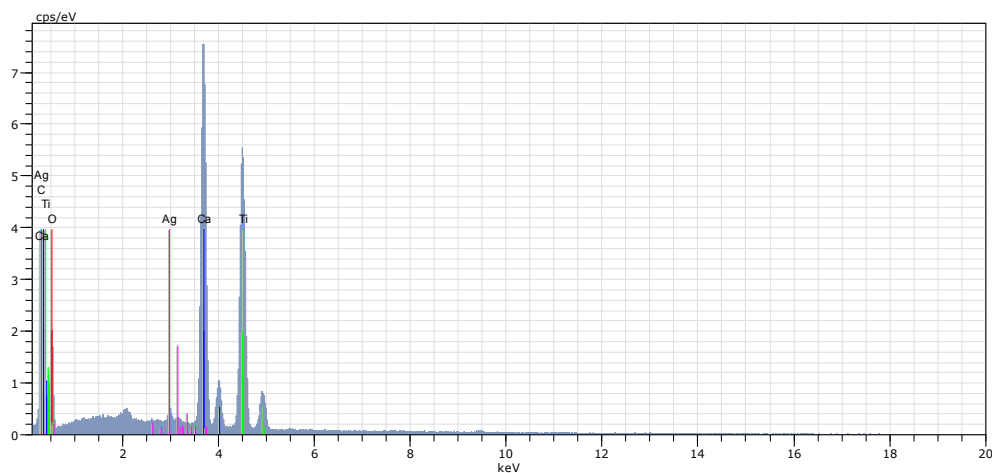
Fig. S4 EDSspectrum ofPr³⁺:CaTiO₃@Ag

Fig. S3 and Fig. S4 are respectively the elemental mapping and the EDSspectrumofPr³⁺:CaTiO₃@Ag. Fig. S3 and Fig. S4 show that the surface ofPr³⁺:CaTiO₃@Agis composed of Ag, Ca, Ti, and O elements. TheAg element comes from Ag nanoparticles connected on the surface of Pr³⁺:CaTiO₃.

2.3Enantioselective current ofPr³⁺:CaTiO₃@Ag@L-cysteine

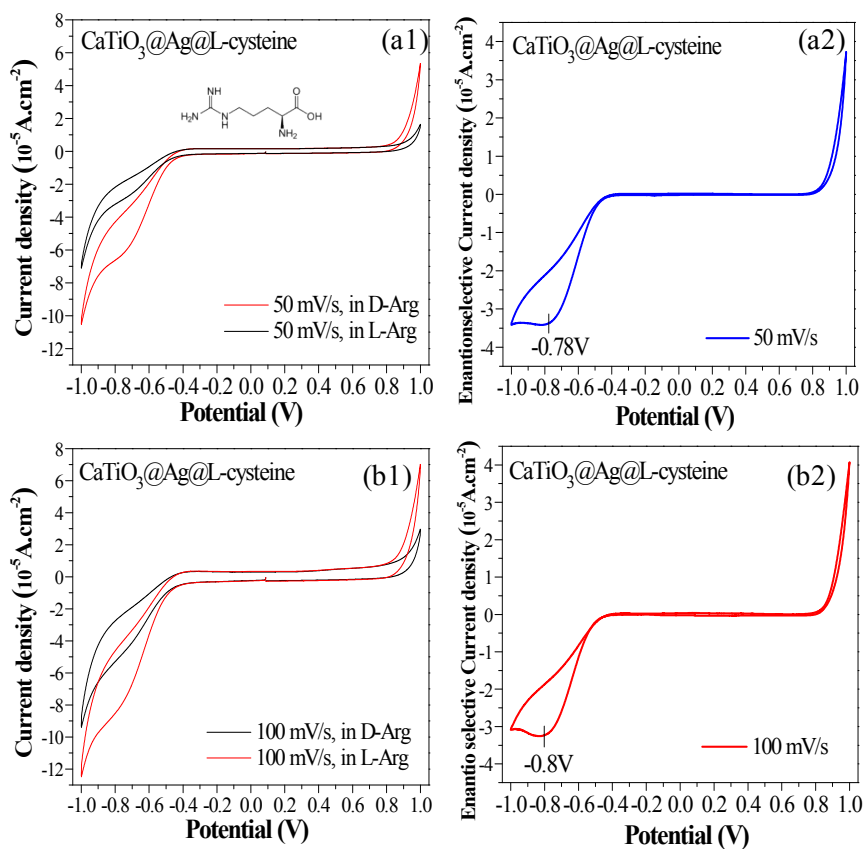**Fig. S5** The CV characteristics of L-Arginine and D-Arginine in 50mM KCl
(a) CV of Pr³⁺:CaTiO₃@Ag, 50mV/s (b) Enantioselective current of Pr³⁺:CaTiO₃@Ag, 50mV/s

(c) CV of Pr^{3+}:CaTiO$_3$@Ag@L-cysteine, 50mV/s (d) Enantioselective current of Pr^{3+}:CaTiO$_3$@Ag@L-cysteine, 50mV/s; (e) CV of Pr^{3+}:CaTiO$_3$@Ag@L-cysteine, 100mV/s (f) Enantioselective current of Pr^{3+}:CaTiO$_3$@Ag@L-cysteine, 100mV/s

2.4 Detection sensitivity of Pr^{3+}:CaTiO$_3$@Ag@L-cysteine for Arginine enantiomers

Fig. S5 shows enantioselective behavior of the working electrodes coated by CaTiO$_3$:Pr^{3+}@Ag@L-cysteine. Fig. S5 (a2) is calculated from Fig. S5 (a1), while Fig. S5 (b2) is calculated from Fig. S5 (a2). The calculating is by subtracting the CV current in D-Arginine/KCl solution from that in L-Arginine/KCl solution, namely,

$$\text{Enantioselective Current} = I_{\text{L-Arginine}} - I_{\text{D-Arginine}}$$

where $I_{\text{D-Arginine}}$ means the CV current in D-Arginine/KCl solution while $I_{\text{L-Arginine}}$ means the CV current in L-Arginine/KCl solution.

As shown in Fig. S5(a2), CaTiO$_3$:Pr^{3+}@Ag@L-cysteine has the best enantioselective performance at -0.78V with the scanning rate of 50 mV when the potential is negative.100mV/s results in higher CV current on CaTiO$_3$:Pr^{3+}@Ag@L-cysteine electrode (Fig. S5 (b1)), while its best enantioselective performance occurs at-0.8V potential (see Fig. S5 (b2)).

To evaluate the sensitivity of Pr^{3+}:CaTiO$_3$@Ag@L-cysteine for Arginine, we explored the electrochemical behavior of Pr^{3+}:CaTiO$_3$@Ag@L-cysteine in L- and D-Arginine aqueous solution at the concentration of 5 mM, 1 mM, 0.1 mM, and 0.01 mM in our set-up. As shown in Fig. S6(a-d), when Arginine concentration was higher than 0.01 mM, CV current in L-Arginine solution (I_L)at -0.78V was larger than that in D-Arginine solution (I_D), which stems from the **CISS**-induced electrons transporting favor of Pr^{3+}:CaTiO$_3$@Ag@L-cysteine for L-Arginine.

As for this work, the sensitivity could be calculated based on Fig. 3(b) and Fig. S6 (a-d) via the following equation:

$$\text{Sensitivity} = (I_L - I_D)/ I_L$$

As discussed in the manuscript, Pr^{3+}:CaTiO$_3$@Ag@L-cysteine exhibited the best chiral identifying performance at -0.78V when scanning rate is 50 mV/s. So herein, we choose the CV current for calculation.

Tab. S2 summarized of the enantio-selective current (I_L, I_D) and sensitivity of Pr^{3+}:CaTiO$_3$@Ag@L-cysteine for L- and D-Arginine at different concentration. The difference between I_L and I_D is very small when Arginine concentration was 0.01 mM. One could not

identify L- or D- enantiomer. Therefore, detection limit of Pr^{3+}:$CaTiO_3$@Ag@L-cysteine for the enantiomers of Arginine is .about 0.1 mM. Though the detection sensitivity of Pr^{3+}:$CaTiO_3$@Ag@L-cysteine is not as high as some other enantio-selective sensors, the novel results in this work unveil the potential of combining the advantages of ***CISS*** effectand persistent luminescent materials for chiral sensing in a convenient way. Besides, in future, its sensitivity and efficiency could be improved by modifying the L-cysteine supramolecular structure and the Ag NPs distribution on its surface.
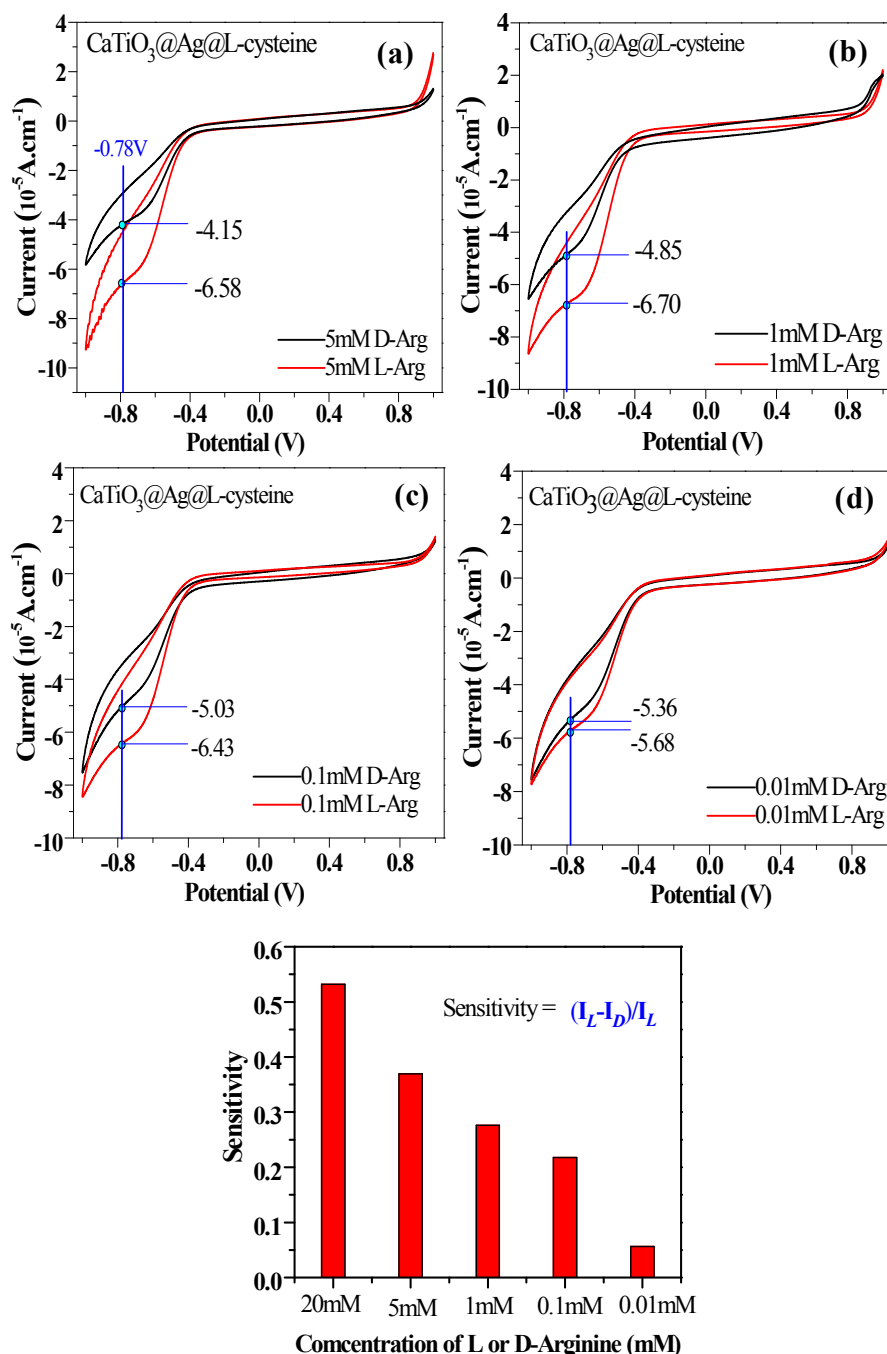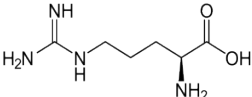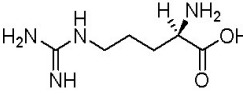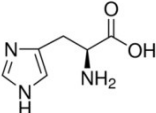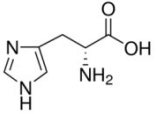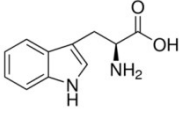

Fig. S6 Electrochemical response of Pr^{3+}:$CaTiO_3$@Ag@L-cysteine in L- and D-Arginine aqueous solution at the concentration of (a) 5 mM, (b) 1 mM, (c) 0.1 mM, and (d) 0.01 mM
(e) Sensitivity calculated from Fig. S6(a-d)

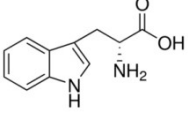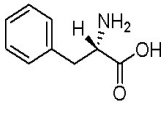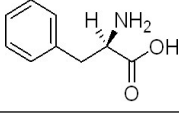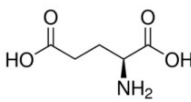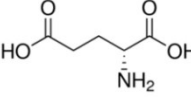**Tab. S2** Summarization of the enantio-selective current (I_L, I_D) and sensitivity of Pr^{3+}:$CaTiO_3$@Ag@L-cysteine for L- and D-Arginine, based on Fig. 3(b) and Fig. S6 (a-d)

Concentration of L- or D-Arginne	I_L(at -0.78V)	I_D(at -0.78V)	Sensitivity (I_L - I_D)/ I_L
20 mM (see Fig. 3(b))	-6.45	-3.02	0.53
5 mM (see Fig. S6(a))	-6.58	-4.15	0.37
1 mM (see Fig. S6(b))	-6.70	-4.85	0.28
0.1 mM (see Fig. S6(c))	-6.43	-5.03	0.22
0.01 mM (see Fig. S6(d))	-5.68	-5.36	0.056

2.5 Selectivity of Pr^{3+}:$CaTiO_3$@Ag@L-cysteine for Arginine enantiomers

Tab. S3 Structural formula of Amino acid used for selectivity detection

Amino acid	Structural formula	Molecular formula
L-Arginine		$C_6H_9N_3O_2$
D-Arginine		$C_6H_9N_3O_2$
L-Histidine		$C_6H_9N_3O_2$
D-Histidine		$C_6H_9N_3O_2$
L-Tryptophan		$C_{11}H_{12}N_2O_2$
D-Tryptophan		$C_{11}H_{12}N_2O_2$
L-Phenylalanine		$C_9H_{11}NO_2$
D-Phenylalanine		$C_9H_{11}NO_2$

L-Glutamic acid		$C_5H_9NO_4$
D-Glutamic acid		$C_5H_9NO_4$
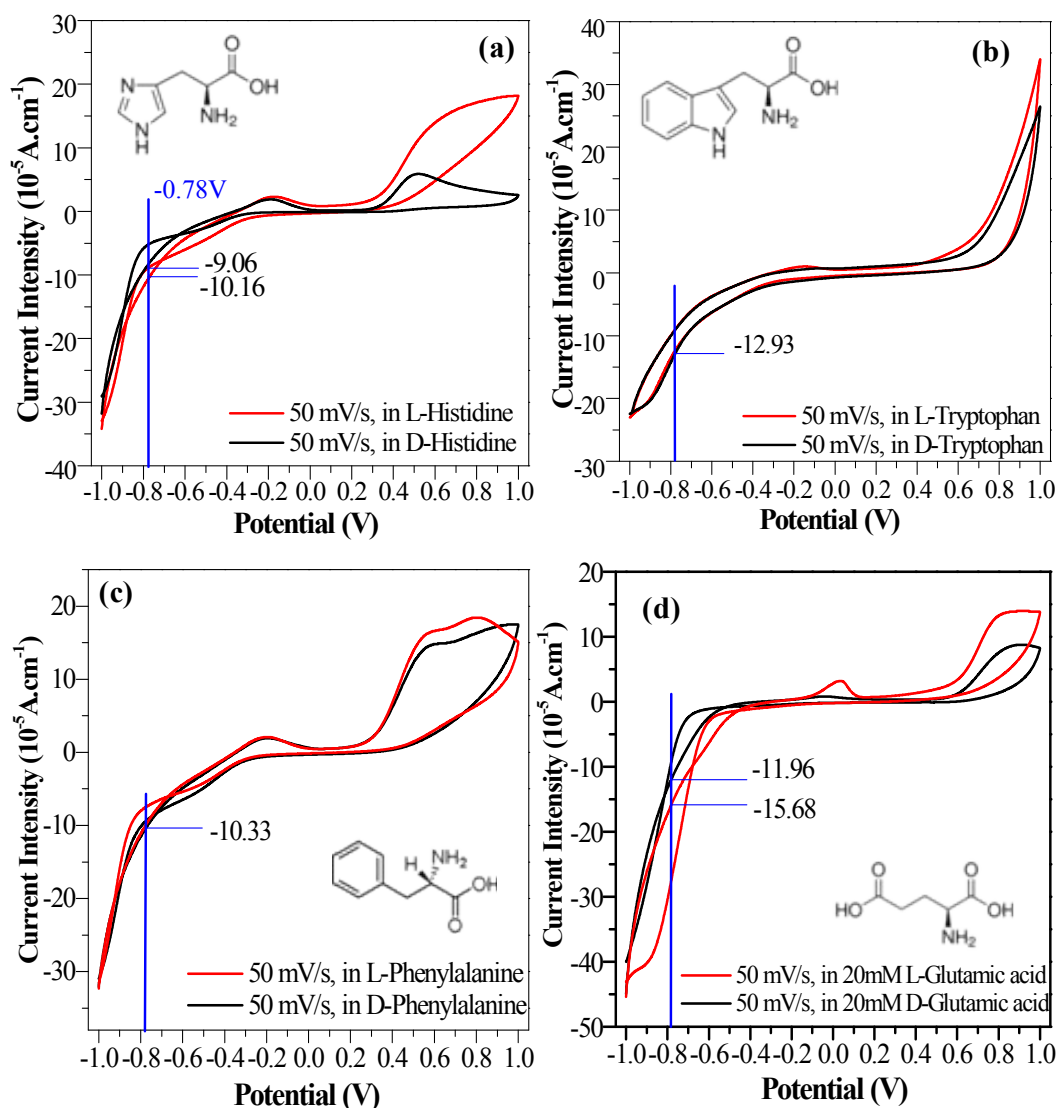
Fig. S7 Electrochemical response of Pr^{3+}:$CaTiO_3$@Ag@L-cysteine in electrolytes contain 50 mM KCl and 20 mM L- and D-amino acids of (a) Tryptophan, (b) Histidine, (c) Phenylalanine, and (d) Glutamic acid

We tested other four D- and L-amino acids including Histidine, Glutamic acid, Phenylalanine, and Tryptophan in this set-up. Fig. S7 shows the electrochemical response of Pr^{3+}:$CaTiO_3$@Ag@L-cysteine for those amino acids.

As shown in Fig. S7, the Pr^{3+}:$CaTiO_3$@Ag@L-cysteine exhibited higher selectivity towards Arginine, compared with Histidine, Tryptophan and Phenylalanine. Unlike in L- and D-Arginine

(Fig. 3(b)), CV differences at negative potential (especially -0.78V) were very small in the enantiomer solution of L- and D-Histidine (Fig. S7(a)), L- and D-Tryptophan (Fig. S7(b)), L- and D-Phenylalanine (Fig. S7(c)), demonstrating that the Pr^{3+}:CaTiO$_3$@Ag@L-cysteine has no chiral favour for the three amino acids at negative potential in terms of charge transporting. In other words, the Pr^{3+}:CaTiO$_3$@Ag@L-cysteine prefers to identify the enantiomers of L- and D-Arginine rather than that of Histidine, Tryptophan and Phenylalanine at negative potential.

Furthermore, the Pr^{3+}:CaTiO$_3$@Ag@L-cysteine also exhibited chiral identifying performance at negative potential towards L- and D-Glutamic acid (Fig. S7(d)). Considering that both Arginine and Glutamic acid have linear configuration, the result indicates that Pr^{3+}:CaTiO$_3$@Ag@L-cysteine is more efficient in enantiomerselective sensing of linear molecules. Maybe the steric hindrance of their ring groups of Histidine, Tryptophan and Phenylalanine molecules to some extent prevented their contacting with Pr^{3+}:CaTiO$_3$@Ag@L-cysteine surface, so charge transporting between them was not as efficient as that with linear molecules like Arginine and Glutamic acid, thus ***CISS*** effect became less effective for enantio-selective sensing of chiral molecules with ring groups in our set-up.

2.6 The stability of sulfur atoms on Pr^{3+}:CaTiO$_3$@Ag@L-cysteine
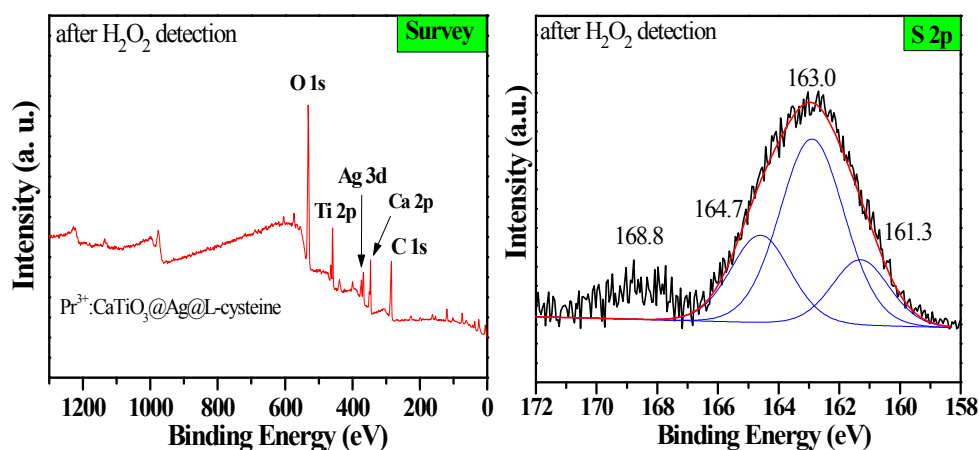
Fig. S8 (a) XPS survey and **(b)** S 2p spectrum of Pr^{3+}:CaTiO$_3$@Ag@L-cysteine after the hydrogen peroxide production test

Actually, the sulfur compounds coordinate strongly to silver, which could be robust even over one year without tarnishing [S1]. Besides, many works reported high stability of self-assembled organic monolayers on mental or inorganic surface as those molecules cross-linked to the surface and some molecular parts interlocked with each other [S2,S3]. Given that, in our work,

when those L-cysteine molecules self-assembled on the surface, they were cross-linked to the surface and interlocked with each other to form robust supramolecular structure with one handedness in which their short alkyl ends faced outside while the sulfur-silver bonds were shielded inside, thus exhibiting higher stability than free sulfur compounds in the presence of hydrogen peroxide. Therefore, large amounts of sulfur atoms should still be stable during hydrogen peroxide production.

Above hypothesis is proved by the S 2p XPS spectrum of Pr^{3+}:CaTiO$_3$@Ag@L-cysteine surface after the hydrogen peroxide production test. Fig. S8(a),(b) are the XPS survey and S 2p XPS spectrum of Pr^{3+}:CaTiO$_3$@Ag@L-cysteine surface after the hydrogen peroxide production test. As shown in Fig. S8(b), the peak at 164.7 eV is due to C-S-C bonds, while the broad peak at 168.8 eV belongs to oxidized sulfur groups like SO_4^{2-}[S4]. They mainly come from the 0.1 M Na$_2$SO$_4$ electrolyte in which the hydrogen peroxide production test was conducted. Meanwhile, the appearance of SO_4^{2-} groups indicates small amount of sulfur atoms might be oxidized to produce sulfur-contained oxide. In Fig. S8(b), the S 2p$_{3/2}$ peak at 161.3 eV and S 2p$_{1/2}$ peak at 163.0 eV correspond to the sulfur ions of S^{2-} state, which provide evidences that large amounts of sulfur atoms from L-cysteine were still stable after the test of hydrogen peroxide production. The robust L-cysteine molecular layer played key role in inhibiting the hydrogen peroxide production via spin-selection.

2.6 Short review and comparison ofPr^{3+}:CaTiO$_3$@Ag@L-cysteine with other chial senaors

Until now, many techniques have been reported for enantio-selective identifying the L- and D-isomers of amino acids, like electrochemical techniques based on molecularly imprinted polymers (MIP) sensor or conducting polymers [S5], chiral mass chemical sensor based on quartz crystal microbalance[S6], chiral optical sensor[S7], and Enzymatic biosensors [S8]. Those techniques exhibited great potential in enantio-selectively sensing the enantiomers of Trptophan, Glutamic Acid, alanine, and Lysine.

However, as to *Arginine*, there are very few studies concerning enantio-selective recognition for its*enantiomers* at present. We listed related studies in Tab.S4. Li et al. reported chiral recognition of L- and D-Arginine on Label-Free PET (polyethylene terephthalate) nanochannel with the aids of BSA (bovine serum albumin) [S9]. Ionic current differential (I_L - I_D) was recorded as detection Signal. Current differential was respectively 0.5nA, 0.7nA and 1.0nA for 0.1mM,

0.5mM and 1mM enantiomer solution, while the detection limit was 0.1mM. Such method is simple, easy, fast-response, low-cost and available in liquid system. Quartz Crystal Microbalance (QCM) technique is also a useful technique for detecting L- and D-Arginine, and the detection limit can achieve 0.38/1.29 μM with chiral calix[4]arene 5 as sensor[S2]. Though the CCC-QCM method has high accuracy, high sensitivity, low detection limit, it requires expensive equipment QCM and its experimental operation is complex. Compared with above methods, enantio-selective sensing with Pr^{3+}:$CaTiO_3$@Ag@L-cysteineis an efficient,convenient and economic way to identify L- and D-Arginine. Furthermore, this method exhibited fast response and nice selectivity for Arginine rather than Tryptophan, Histidine, and Phenylalanine. Though its detection limit was about 0.1mM, not low enough, that could be improved by modifying the L-cysteine supramolecular structure and the Ag NPs distribution on its surface.

Tab. S4 Studies reported for chiral recognition of ***L- and D-Arginine*** enantiomers

Chiral sensor/Material	Detection Signal	Detection Limit	Advantages	Disadvantages
Label-free***PET***nanochannel with ***BSA*** [S5]	Ionic Current differential (I_L - I_D) 0.5nA, 0.7nA and 1.0nA for 0.1mM, 0.5mM and 1mM enantiomer solution, respectively	0.1mM	◆ Simplicity ◆ easy operation ◆ fast response ◆ Availability in liquid system ◆ Low cost	Detection limit need to be lowered down
chiral calix[4]arene 5 coated QCM sensor (CCC-QCM)[S2]	Quartz Crystal Microbalance (QCM) technique	0.38/1.29 μM	◆ High accuracy ◆ High sensitivity ◆ Low detection limit	◆ Expensive equipment ◆ complexity
Pr^{3+}:$CaTiO_3$@Ag@L-cysteine	CV Current differential (I_L - I_D)	0.1mM	◆ Simplicity ◆ easy operation ◆ fast response ◆ Availability in liquid system ◆ Low cost ◆ High selectivity	Detection limit need to be lowered down

PET: polyethylene terephthalate

BSA: bovine serum albumin

I_L: ionic current for L-Arginine

I_D: ionic current for D-Arginine

Additionally, there are some studies concerning chiral separation of L- and D-Arginine. For

instance, Schwaneberg et al. reported chiral separation of D-/L-arginine racemate by a chiral channel protein (FhuAF4), whose enantioselectivity (E-value) was 1.92 and enantiomeric excess percentage (ee %) of 23.91 at 52.39 % conversion[S10]. Han et al. realized chiral separation of L- and D- enantiomer of Arginine in in human serum by LC−MS/MS chiral separation (LC, liquid chromatography; MS, mass spectrometry) with CROWNPAK CR-I(+) column[S11]. Their chiral separation limit was 1.5×10^{-5} mM for L-Arginine. Since chiral sensing and chiral separation are different issues, we do not discuss them in detail and compare them with our method.

Reference

[S1] A.Ulman, *J. Mat. Ed.* 1989, 11, 205.

[S2] A.Ulman, *Chem. Rev.*1996, **96**, 1533–1554

[S3] N.Tliman, A.Ulman,J. S. Schildkrant, T. L.Penner, *JACS*, 1988, **111**, 6136-6144.

[S4] W. Zhang, K. Banerjee-Ghosh, F. Tassinari, R. Naaman, *ACS Energy Lett.,* 2018, **3**, 2308–2313.

[S5]M. P. Tiwari, A. Prasad, *Analytica Chimica Acta* 2015, **853**, 1–18.

[S6] F. Temel, S. Erdemir, E. Ozcelik, B. Tabakci, M. Tabakci, *Talanta* 2019, **204**, 172–181.

[S7]J. Lin, Q. S. Hu, M. H. Xu, L. Pu, *JACS*, 2002, **124**, 2088-2089.

[S8]W. W. Zhao, J. J. Xu, H. Y. Chen, *Biosens. Bioelectron.* 2017, **92**, 294-304.

[S9] Z. Y. Sun,F. Zhang,X. Y. Zhang,D. M. Tian,L. Jiang, H. B. Li, *Chem. Commun*., 2015, **51**, 4823-4826.

[S10] D. Anand,G. V. Dhoke,J. Kinzel,T. M. Garakani,M. D. Davari,M. Bocola,L. Zhua, U. Schwaneberg, *Chem. Commun.*, 2019, **55**, 5431-5434.

[S11] M. Han, M. Y. Xie, J. Han, D. Y. Yuan, T. Yang, Y. Xie, *Anal. Bioanal. Chem.* 201, **410**, 2517-2531.

[S12] A. Alzahrani, D. Barbash and A. Samokhvalov, J. Phys. Chem. C, 2016, **120**, 19970–19979.